Journal of the European Ceramic Society 7 (1991) 185–195

The System Y_2O_3–Sc_2O_3–ZrO_2: Phase Characterisation by XRD, TEM and Optical Microscopy

F. T. Ciacchi, S. P. S. Badwal & J. Drennan

CSIRO, Division of Materials Science and Technology, Normanby Road, Locked Bag 33, Clayton 3168, Victoria, Australia

(Received 16 July 1990; Revised version received 30 October 1990; accepted 5 November 1990)

Abstract

The phase assemblage in the ternary system Y_2O_3–Sc_2O_3–ZrO_2 has been investigated as a function of the Sc_2O_3/Y_2O_3 ratio for several compositions with a constant total stabilizer ($Y_2O_3 + Sc_2O_3$) content of 8 mol%, using X-ray diffraction, transmission electron and optical microscopy. Considerable twinning was observed in as-sintered specimens with higher scandia content ($Sc_2O_3/Y_2O_3 \geq 5/3$). These compositions were indexed as having tetragonal symmetry. The twinning is associated with the formation of a dopant rich tetragonal phase (designated as the t'-ZrO_2 phase) as a result of diffusionless transformation on cooling the material from the sintering temperature at which it had a cubic symmetry. On annealing Sc_2O_3-rich compositions at 1000°C for 2000 h, twinning disappeared and the specimens consisted of cubic matrix with fine precipitates of a low-dopant tetragonal phase (t-ZrO_2) dispersed uniformly. The cubic matrix had a slightly higher dopant content than the corresponding t'-phase. The Y_2O_3-rich compositions in the as-sintered form had cubic symmetry and showed no twinning. On annealing, they decomposed to t-ZrO_2 precipitates plus a cubic solid-solution matrix richer in the dopant. All the eight Y_2O_3/Sc_2O_3 compositions studied were in the two-phase field at the annealing temperature.

Im Dreistoffsystem Y_2O_3–Sc_2O_3–ZrO_2 wurden die Phasenbeziehungen für mehere Zusammensetzungen mit einem Gehalt von jeweils 8 Mol.% ($Y_2O_3 + Sc_2O_3$) in Abhängigkeit des Sc_2O_3/Y_2O_3-Verhältnisses mittels Röntgenbeugung, Transmissionselektronenmikroskopie und optischer Mikroskopie untersucht. In gesinterten Proben mit hohem Sc_2O_3-Gehalt ($Sc_2O_3/Y_2O_3 \geq 5/3$) konnte eine ausgeprägte Zwillingsbildung festgestellt werden. Diesen Zusammensetzungen konnte eine tetragonale Struktur zugeordnet werden. Die Zwillingsbildung wird mit der Bildung einer hoch dotierten tetragonalen Phase (der t'-ZrO_2-Phase) in Zusammenhang gebracht, die sich während des Abkühlens von der Sintertemperatur durch eine diffusionslose Umwandlung aus einer Phase mit kubischer Struktur bildet. Eine Glühbehandlung der Sc_2O_3-reichen Proben bei 1000°C für 2000 h führte zum Verschwinden der Zwillinge. Die Proben wiesen eine kubische Matrix mit homogen verteilten, gering dotierten, kleinen tetragonalen Teilchen (t-ZrO_2) auf. Die kubische Matrix wies eine etwas höhere Dotierung auf, als die entsprechende t'-Phase. Die Y_2O_3-reichen Zusammensetzungen hatten nach dem Sintern kubische Struktur und wiesen keine Zwillingsbildung auf. Nach der Glühbehandlung bildeten sich t-ZrO_2-Teilchen in einer kubischen Matrix mit hoher Dotierung. Alle acht untersuchten Y_2O_3/Sc_2O_3 Zusammensetzungen lagen bei der Glühbehandlung im Zweiphasenfeld.

On a étudié par diffraction X, par microscopie à transmission et par microscopie optique l'ensemble des phases du système ternaire Y_2O_3–Sc_2O_3–ZrO_2 en fonction du rapport Sc_2O_3/Y_2O_3, pour différentes compositions, la teneur totale en stabilisateur ($Y_2O_3 + Sc_2O_3$) étant égale à 8% molaires. Les échantillons à teneur à élevée en oxyde de scandium ($Sc_2O_3/Y_2O_3 \geq 5/3$) présentaient, après frittage, un maclage très important. Ces compositions possèdaient une symétrie tétragonale. Ce maclage est associé à la formation d'une phase tétragonale riche en dopant (appelée phase t'-ZrO_2) résultant de la transformation non diffusionnelle se produisant lors du refroidissement du matériau à partir de la témperature de frittage, pour laquelle il présente une symétrie cubique. Lors d'un recuit à 1000°C pendant 2000 h, le maclage des compositions riches en Sc_2O_3

Journal of the European Ceramic Society 0955-2219/91/$3.50

disparaissait et les échantillons étaient constitués d'une matrice cubique avec de fins précipités de phase tétragonale pauvre en dopant (t-ZrO_2) dispersés uniformément. La matrice cubique possèdait une teneur en dopant légèrement plus élevée que la phase t' correspondante. Les compositions riches en Y_2O_3 présentaient, après frittage, une symétrie cubique et n'étaient pas maclées. Lors du recuit, elles se décomposaient en précipités t-ZrO_2 dans une matrice de solution solide plus riche en dopant. Les huit compositions Y_2O_3/Sc_2O_3 étudiées étaient à la température de recuit dans le domaine biphasé.

1 Introduction

Over the last ten to fifteen years there has been an increasing interest in zirconia (ZrO_2) based ceramic materials.[1] Zirconia is used mainly in the abrasive, refractory, and paint and enamel manufacturing industries. However, more recently numerous high technology applications have emerged. These applications of zirconia-based ceramics take advantage of their unique thermal, mechanical and oxygen-ion conducting properties.

Amongst the number of aliovalent oxides which can stabilize the ZrO_2 cubic structure are yttria (Y_2O_3) and scandia (Sc_2O_3), whose binary solid solutions are attractive because of their good overall electrolyte properties. Interest in these materials stems from the ability of Y_2O_3 to stabilize ZrO_2 extremely well and the high oxygen-ion conductivity demonstrated by the Sc_2O_3-stabilized ZrO_2.[2,3] An understanding of the phase equilibria of these zirconia systems is fundamental to the use of such materials as solid electrolytes.

Both yttria–zirconia and scandia–zirconia binary-phase equilibria systems are plagued by uncertainty. In the yttria–zirconia system, as with many binary systems, early work produced conflicting results. The phase diagram work of several authors has been summarized by Yoshimura[4] for the yttria–zirconia system. The phase diagram due to Scott[5] appears to be the most reliable. Even more uncertainty remains concerning the Sc_2O_3–ZrO_2 system;[6,7] the system is quite complex in that it has eight phases reported, seven of which appear in the composition range 0 to 25 mol% Sc_2O_3. Difficulties in the establishment of the phase equilibria of this system are associated with the sluggishness with which solid state transformations take place. This is evident as reported by Thornber *et al.*,[6] in that a number of phases appear, resulting from different material preparation techniques.

Amongst various zirconia systems studied, the highest conductivity has been reported for 8 mol% Sc_2O_3–ZrO_2,[2,3] whereas about 8 mol% Y_2O_3 is required to stabilize the cubic phase. In this paper the phase assemblage in the homogeneously mixed Sc_2O_3–Y_2O_3–ZnO_2 compositions is investigated by X-ray diffraction, transmission electron microscopy (TEM) and optical microscopy. The total stabilizer content was kept constant at 8 mol% and the Y_2O_3/Sc_2O_3 ratio was varied between the two extremes. In another paper[8] the results of conductivity measurements as a function of time, temperature and the impurity content are reported.

2 Experimental Procedure

Materials used were Y_2O_3 (Lindsay Rare Earth Chemicals, 99·9 wt% pure), Sc_2O_3 (Australian Mineral Development Laboratories, 99·5 wt% pure) and ZrO_2 containing 2 wt% HfO_2 (Harshaw Chemical Company, 99·7 wt% pure). The LOI at 1100°C were 0·96, 0·94 and 1·06 wt% respectively. The silica content was 0·6 wt% in Sc_2O_3 and 0·03 wt% in ZrO_2. These materials were used for preparing the mixed oxide specimens FC01 and FC02 (Table 1). The oxide powders were thoroughly mixed using a plastic container and acrylic balls, calcined, isostatically pressed into rods and sintered (Table 1).

For preparing coprecipitated powders, basic carbonate of zirconium (Magnesium Elektron) with silica content of 0·18 wt% was used. The nitrate solutions were prepared from yttrium and scandium oxides and the basic carbonate of zirconium by dissolving them separately in nitric acid. Coprecipitation was performed by adding the solution containing the required amounts of metal nitrates to ammonium hydroxide. The coprecipitate was filtered and washed with deionized water until free of chloride and nitrate. The filter cake was dispersed in acetone using an ultrasonic bath, filtered and dried in a vacuum oven at 60°C. During coprecipitation a nitrogen atmosphere was maintained over the solution and the precipitate. The coprecipitated powders were milled with isopropanol for 3 h using either a plastic (specimens R3 and R5) or a glass-bonded teflon (specimens S1 to S8) container and high-purity alumina balls. The slurry was dried and calcined. The powder was then pressed isostatically into rectangular bars and sintered. Details of the specimen preparation techniques, nomenclature and calcination and sintering temperatures are given in Table 1 and measured specimen densities in Table 2.

Coprecipitated specimens were sintered in air at

Table 1. Details of specimen preparation

Specimen	*Specimen composition*[a] (*x mol% Y_2O_3*)	*Calcination temperature* (*T*, °C)[b]	*Sintering temperature* (*T*, °C)[c]
S1	1	700	1 750
S2	2	700	1 750
S3	3	700	1 750
S4	4	700	1 750
S5	5	700	1 750
S6	6	700	1 750
S7	7	700	1 750
S8	8	700	1 750
R3	3	700	1 750
R5	5	700	1 750
FC01[d]	4	700	1 700, 1 850[e]
FC02[d]	2	1 100	1 700, 1 850[e]
AS1	1	—	—[f]
AS2	2	—	—[f]
AS3	3	—	—[f]
AS4	4	—	—[f]
AS5	5	—	—[f]
AS6	6	—	—[f]
AS7	7	—	—[f]
AS8	8	—	—[f]

[a] *x* mol% Y_2O_3 in *x* mol% Y_2O_3 + (8-*x*) mol% Sc_2O_3 + 92 mol% ZrO_2.
[b] For 1 h.
[c] For 15 h.
[d] Except for these specimens which were prepared by mixing oxide powders, all other specimens were prepared by the coprecipitation technique.
[e] For 15 h at 1700°C then 5 h at 1850°C.
[f] Coprecipitated and sintered specimens S1–S8 after annealing at 1000°C for 2000 h. The composition as per S1–S8 respectively. The prefix 'A' in the nomenclature indicates annealing.

Table 2. Details of specimen densities

Specimen	*Specimen composition* (*x mol% Y_2O_3*)[a]	*Specimen density* ($g\,cm^{-3}$; *% of theoretical*)	*Theoretical density* ($g\,cm^{-3}$)
S1	1	5·63 (96·2)	5·85
S2	2	5·64 (96·1)	5·87
S3	3	5·61 (95·3)	5·89
S4	4	5·66 (95·6)	5·92
S5	5	5·53 (93·1)	5·94
S6	6	5·55 (93·1)	5·96
S7	7	5·64 (94·3)	5·98
S8	8	5·77 (96·2)	6·00
AS1	1	5·61 (95·9)	5·85
AS2	2	5·67 (96·6)	5·87
AS3	3	5·66 (96·1)	5·89
AS4	4	5·68 (96·1)	5·91
AS5	5	5·74 (96·8)	5·93
AS6	6	5·61 (94·1)	5·96
AS7	7	5·71 (95·5)	5·98
AS8	8	5·80 (96·7)	6·00
R3	3	5·50 (93·2)	5·89
R5	5	5·68 (95·6)	5·94
FC01	1	5·33 (91·1)	5·85
FC02	2	5·20 (88·6)	5·87

[a] *x* mol% Y_2O_3 in *x* mol% Y_2O_3 + (8-*x*) mol% Sc_2O_3 + 92 mol% ZrO_2.

1750°C in a tube furnace (heating and cooling rate 300°C h^{-1}). The mixed oxide specimens were initially sintered at 1700°C but were later given a further heat treatment in the gas-fired furnace at 1850°C to complete the reaction and to achieve increased density. Sections of the as-sintered coprecipitated specimens S1 to S8 were annealed at 1000°C for 2000 h in an ambient air environment (corresponding specimen nomenclature for annealed specimens AS1 to AS8).

Routine phase identification was performed using a diffractometer. For this specimens were crushed and ground to ~200 mesh. Precise lattice parameters for phases present were determined using a Guinier fine focussing camera ($Cu\,K_{\alpha 1}$) on all as-sintered (S1–S8) and annealed at 1000°C for 2000 h (AS1–AS8) specimens prepared by the coprecipitation technique. ThO_2(a_0 = 0·55971 nm), was used as an internal standard. The line positions were measured using a video camera mounted on a travelling stage equipped with a displacement transducer with an accuracy of ±0·005 mm and a resolution of 0·001 mm.

Optical microscopy was performed on as-sintered specimens S1–S8 to investigate grain size distribution, grain boundaries and general phase regions of the specimens. For this specimens were carefully polished and thermally etched at 1500°C in air.

Specimens for TEM investigation were prepared from selected (i) as-sintered, and (ii) annealed (1000°C, 2000 h) coprecipitated materials. A disc measuring 3 mm in diameter was drilled, ground, dimpled to a depth of approximately 100 μm, polished and then ion-beam thinned. To prevent charging in the electron microscope, specimens were coated with a thin layer of carbon. TEM investigations were accomplished using a Philips EM420 analytical transmission electron microscope. An EDAX PV9900 energy-dispersive X-ray analysis system was employed in conjunction with the TEM.

The grain size was measured from optical photomicrographs using the line intercept method. In general, 400–600 intercepts were measured (which corresponds to 100–150 grains, respectively).

3 Results and Interpretation

3.1 Mixed oxide specimens

X-ray diffraction patterns of the mixed oxide specimens heated to 1700°C (15 h) showed the presence of monoclinic zirconia (m-ZrO_2) and a fluorite-related phase. On heating to1850°C (5 h) in air the monoclinic ZrO_2 lines either disappeared or significantly decreased, but preliminary transmission electron microscopy work indicated significant

inhomogeneities. The presence of the m-ZrO_2 in specimens sintered at 1700°C is associated with incomplete phase reaction and compositional inhomogeneities in the mixed oxide specimens.[3] Most of the subsequent work was performed on coprecipitated specimens.

3.2 Coprecipitated specimens

3.2.1 X-ray diffractograms

In the coprecipitated specimens in which the distribution of the yttrium, scandium and zirconium is more uniform, X-ray diffractograms recorded from the surface of all as-sintered specimens sintered at 1750°C clearly indicated that both Y_2O_3 and Sc_2O_3 had reacted with ZrO_2 to form a solid solution. No unreacted stabilizer or monoclinic zirconia were detected in any of the coprecipitated specimens.

X-ray diffractograms of the as-sintered materials of composition 1 mol% Y_2O_3 + 7 mol% Sc_2O_3 + 92 mol% ZrO_2 (S1) and 2 mol% Y_2O_3 + 6 mol% Sc_2O_3 + 92 mol% ZrO_2 (S2) showed clear splitting of the face-centred cubic 200, 220 and 311 peaks, corresponding to the presence of a tetragonal phase. For compositions containing more than 3 mol% Y_2O_3 the splitting was too small to clearly identify the existence of the tetragonal phase. As-sintered Y_2O_3-rich compositions were essentially single-phase materials with the face-centred cubic structure.

The peak positions shifted towards lower 2θ angles with increasing yttrium content. This was expected because, as the yttrium ion is larger than the scandium ion, the cell volume increases with yttrium content.

3.2.2 Guinier

The as-sintered specimens between the composition range 1 mol% Y_2O_3 + 7 mol% Sc_2O_3 + 92 mol% ZrO_2 (S1) and 5 mol% Y_2O_3 + 3 mol% Sc_2O_3 + 92 mol% ZrO_2 (S5) inclusive were indexed as having the tetragonal symmetry. Within this range the degree of tetragonality decreased (indicated by the decreasing difference between the a and c lattice parameters) as the yttria concentration increased (Fig. 1). The remaining as-sintered specimens in this series, with higher yttria concentrations, were indexed as having cubic symmetry.

All the annealed specimens were indexed as having cubic symmetry (Fig. 1); however, the cubic lines were broad, symmetrical and diffuse for compositions which in the as-sintered form exhibited tetragonal symmetry. Annealed specimens (AS6–AS8), which in the as-sintered state had cubic symmetry (specimens S6–S8), exhibited negligible

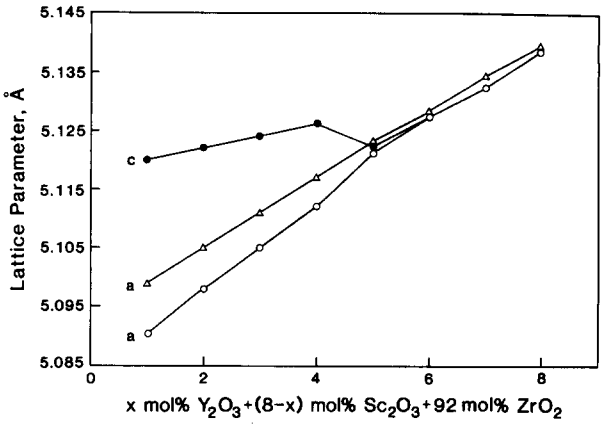

Fig. 1. Plots of lattice parameter(s) versus composition. △, lattice parameter a for annealed specimens; ○, lattice parameter a and ●, lattice parameter c for as-sintered specimens.

cubic line broadening but increased cell parameters. Table 3 gives details of lattice parameters and identified phases of as-sintered and annealed specimens.

Figure 2 shows cell volume–composition plots for as-sintered and annealed specimens. Annealed specimens of low yttria concentration (AS1 and AS2) had smaller cell volumes than corresponding as-sintered specimens (S1 and S2) respectively, whereas annealed specimens with higher yttria concentrations (≥4 mol%) (AS4–AS8) exhibited larger cell volumes compared with the respective as-sintered specimens (S4–S8). At a composition

Table 3. Details of lattice parameters and identified phases of as-sintered and annealed specimens

Specimen	*Lattice parameters (Å; cell volume, Å³)*		
	As-sintered		*Annealed*
	Tetragonal	*Cubic*	*Cubic*
S1	5·090 4 (132·65) 5·119 5	—	
AS1			5·099 2 (132·59)
S2	5·098 1 (133·12) 5·121 9	—	
AS2			5·105 1 (133·05)
S3	5·104 6 (133·50) 5·123 5	—	
AS3			5·110 6 (133·48)
S4	5·111 9 (133·94) 5·125 6	—	
AS4			5·117 4 (134·01)
S5	5·120 7 (134·30) 5·121 7	—	
AS5			5·122 9 (134·45)
S6	—	5·126 8 (134·75)	
AS6			5·128 2 (134·86)
S7	—	5·132 2 (135·18)	
AS7			5·133 7 (135·30)
S8	—	5·137 5 (135·60)	
AS8			5·139 1 (135·73)

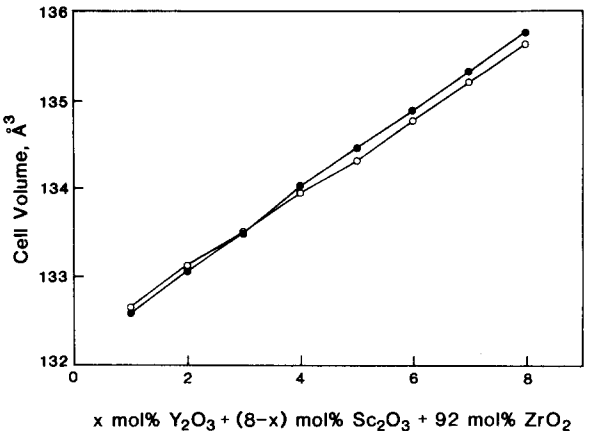

Fig. 2. Plots of cell volume of ○, as-sintered and ●, annealed specimens as a function of composition.

of approximately 3 mol% Y_2O_3 + 5 mol% Sc_2O_3 + 92 mol% ZrO_2 a 'crossover' in the cell volume of the as-sintered tetragonal and annealed cubic symmetry occurred. As a consequence of the anneal the lattice parameter a of the as-sintered tetragonal form increased whilst the lattice parameter c decreased.

Theoretical densities of the various compositions were calculated based on the cell volume determinations and are given in Table 2. The theoretical density increased with increasing Y_2O_3 content.

3.2.3 Optical microscopy and grain size measurements

Figure 3 shows optical micrographs of thermally etched as-sintered, coprecipitated specimens. Several of these specimens exhibited a twinned morphology. The 1 mol% Y_2O_3 + 7 mol% Sc_2O_3 + 92 mol% ZrO_2 (S1) specimen had the highest degree of twinning (Fig. 3(a)), virtually every grain appearing to be completely twinned. The degree and level of twinning decreased as the yttria concentration increased up to a composition of 5 mol% Y_2O_3 + 3 mol% Sc_2O_3 + 92 mol% ZrO_2 (S5). In the S5 specimen only isolated and partially twinned grains were observed. Compositions with higher yttria concentration which had cubic symmetry in the as-sintered state exhibited no twinning.

The average grain size varied from 25 to 39 μm in

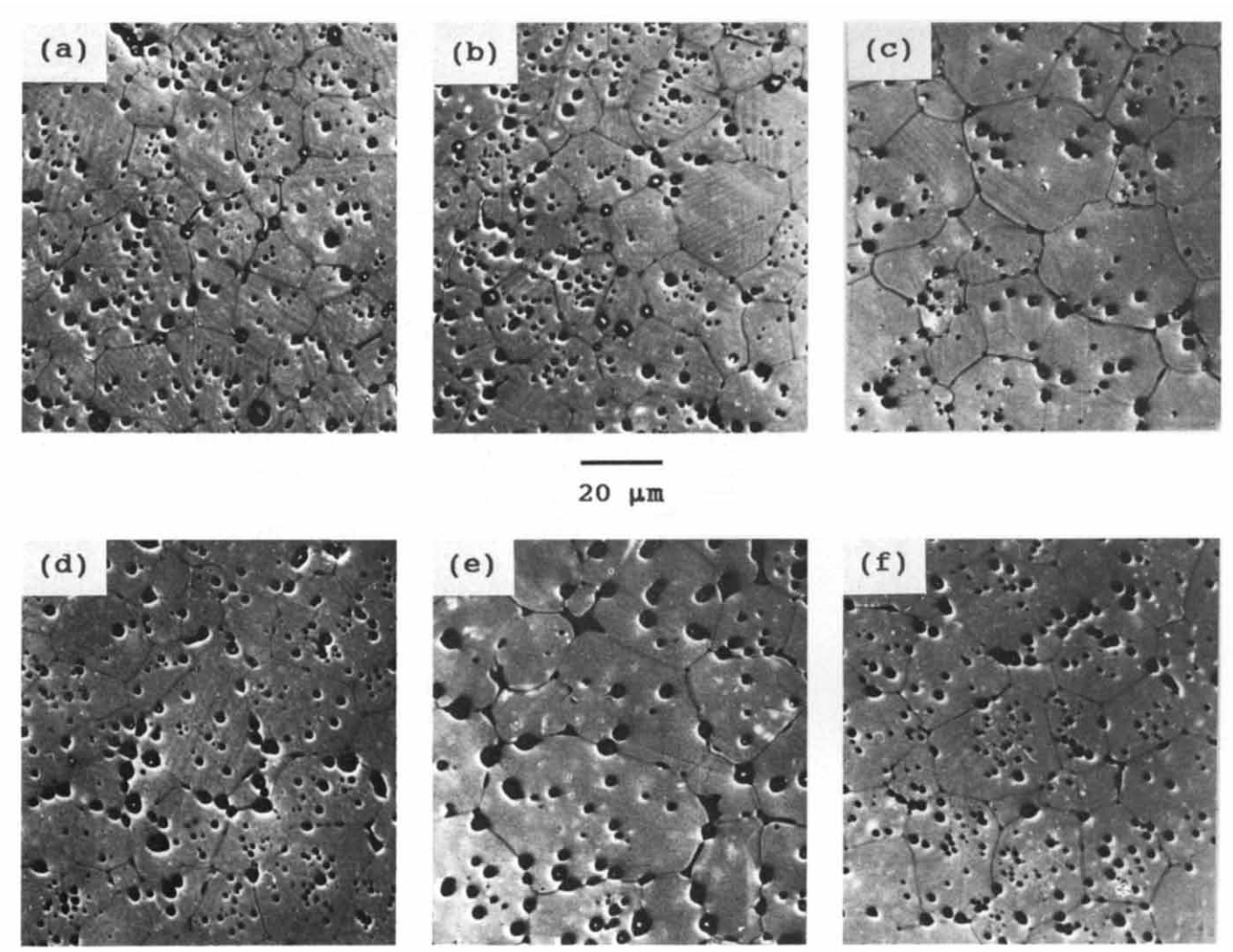

Fig. 3. Optical micrographs of as-sintered specimens: (a) S1; (b) S2; (c) S3; (d) S4; (e) S6; (f) S8.

the as-sintered specimens, with the compositions indexed as cubic (S6, S7 and S8) having the larger average grain size (35–39 μm).

3.2.4 Transmission electron microscopy (TEM)

Bright field transmission electron micrographs were taken of selected as-sintered (Figs 4(a), 5(a) and 6(a)) and annealed (1000°C, 2000 h) specimens (Figs 4(b), 5(b) and 6(b)). For the as-sintered material 1 mol% Y_2O_3 + 7 mol% Sc_2O_3 + 92 mol% ZrO_2 (S1), individual grains of the ceramic showed massive twinning as can be clearly seen in Fig. 4(a). The twinning can not be associated with the presence of monoclinic zirconia as this phase was not detected in any of the as-sintered or annealed coprecipitated specimens by X-ray diffraction, electron diffraction and energy dispersive X-ray analysis. Instead, based on electron diffraction patterns which clearly showed tetragonal symmetry in twinned regions, and X-ray diffraction work described earlier, it is concluded that the sample consists of a dopant-rich tetragonal phase. This phase will be designated as the t'-phase to distinguish it from the low dopant t-ZrO_2 phase. Energy dispersive X-ray analysis revealed a uniform scandium and yttrium distribution throughout the grains at the expected Sc/Y ratio, indicating that there is only a single variant of this dopant-rich tetragonal phase. This type of microstructure (twinning) has been previously reported for yttria–zirconia (5–12 wt.% Y_2O_3) ceramics,[9,10] which had been quenched from annealing temperatures >1550°C and in scandia–zirconia[3,11,12] cooled normally from the sintering temperature. On annealing specimen S1, the nature of the microstructure was seen to change. There the massive twinning was now replaced by a dappled appearance (Fig. 4(b)) within the grains. This type of microstructure is usually observed for zirconia or other similar ceramics and has been reported often; it results from a combination of ion-beam damage and the presence of precipitates. The diagonal line running across the top right of the micrograph in Fig. 4(b) is a grain boundary.

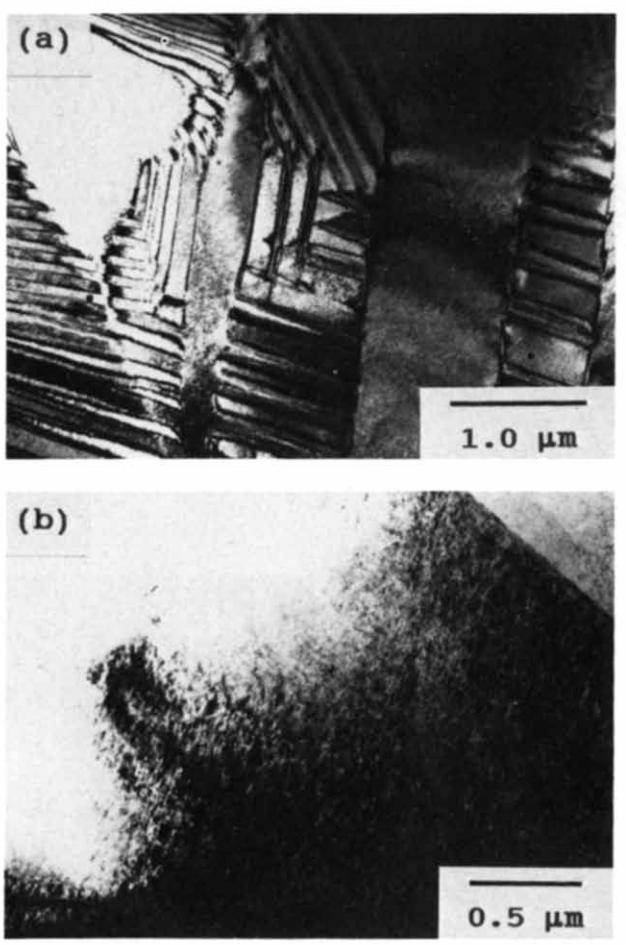

Fig. 4. Transmission electron micrographs (bright field) of 1 mol% Y_2O_3 + 7 mol% Sc_2O_3 + 92 mol% ZrO_2 specimens: (a) as-sintered (S1) and (b) annealed (AS1). The large hole at the top left in (a) is a pore.

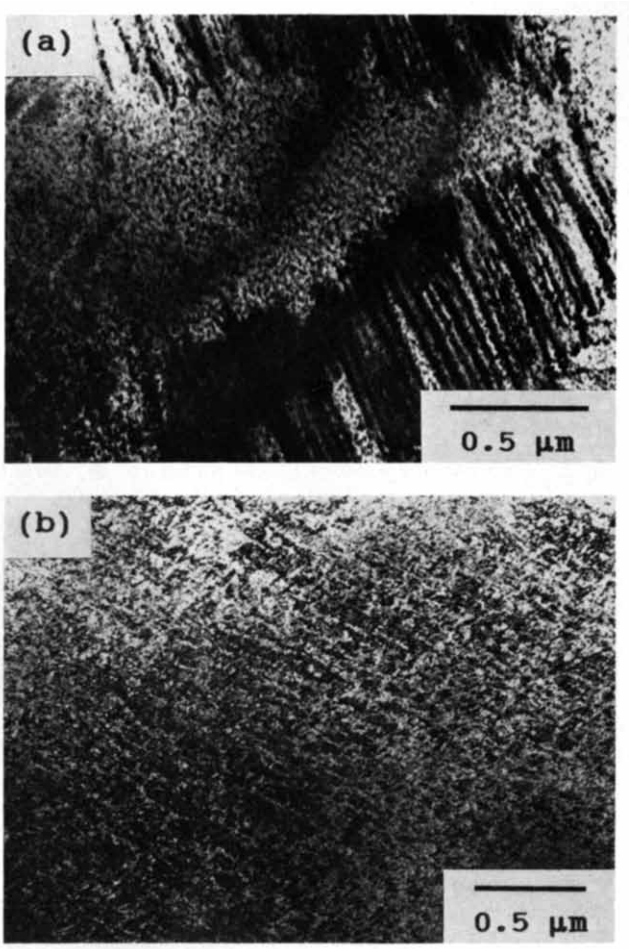

Fig. 5. Transmission electron micrographs (bright field) of 4 mol% Y_2O_3 + 4 mol% Sc_2O_3 + 92 mol% ZrO_2 specimens: (a) as-sintered (S4) and (b) annealed (AS4).

Twinning was also observed in the as-sintered 4 mol% Y_2O_3 + 4 mol% Sc_2O_3 + 92 mol% ZrO_2

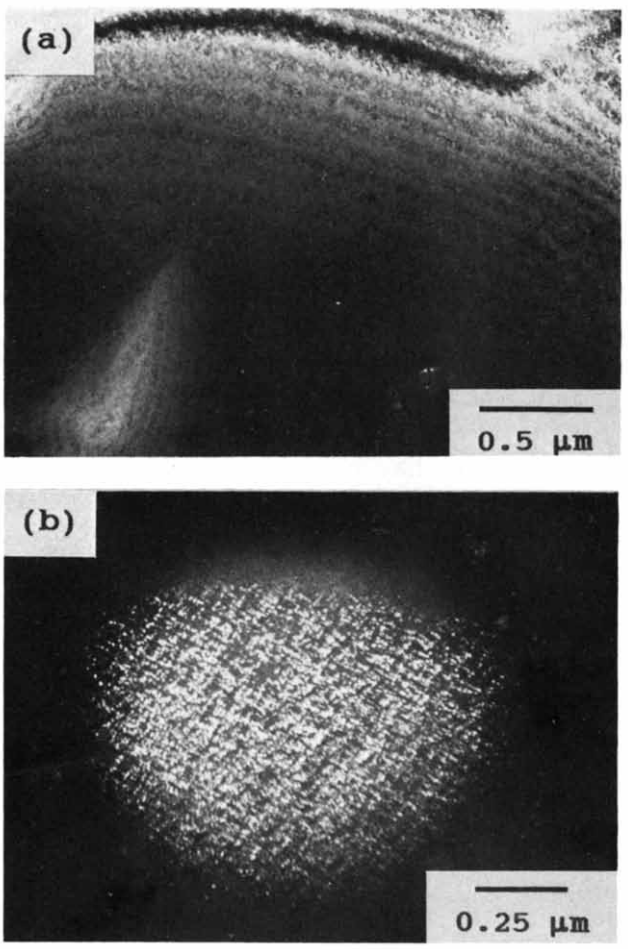

Fig. 6. Transmission electron micrographs of 8 mol% Y_2O_3 + 92 mol% ZrO_2 specimens: (a) as-sintered (S8; bright-field) and (b) annealed (AS8; dark field).

(S4) ceramic material as shown in Fig. 5(a). However, the degree of twinning was not as pronounced as with the higher Sc_2O_3-containing material. This is consistent with optical microscopy observations. As with the 1 mol% Y_2O_3 + 7 mol% Sc_2O_3 + 92 mol% ZrO_2 (AS1) annealed specimen, after annealing the 4 mol% Y_2O_3 + 4 mol% Sc_2O_3 + 92 mol% ZrO_2 (AS4) material also showed no sign of twinning; instead, fine scale 'precipitates' were observed, as shown in Fig. 5(b).

The 8 mol% Y_2O_3 + 92 mol% ZrO_2 (S8) as-sintered specimen had no traces of twinning; instead it had very fine-scale precipitates and/or ion-beam damage which is shown in Fig. 6(a). A dark field transmission electron micrograph (Fig. 6(b)) after annealing the specimen clearly showed precipitates. These precipitates were identified by electron diffraction analysis to consist of approximately 60 Å particles of low-Y_2O_3 containing tetragonal ZrO_2. This phase is commonly referred to as t-ZrO_2.

Further evidence for the formation of t-ZrO_2 precipitates is shown in the dark field transmission electron micrographs of selected annealed specimens in Fig. 7 which show the fine-scale precipitation. In an attempt to determine if tetragonal precipitates would transform under strain, the surface of two annealed specimens 1 mol% Y_2O_3 + 7 mol% Sc_2O_3 + 92 mol% ZrO_2 (AS1) and 8 mol% Y_2O_3 + 92 mol% ZrO_2 (AS8) were ground mechanically. There was no indication of any monoclinic ZrO_2 resulting from the tetragonal to monoclinic transformation induced by the mechanical grinding, suggesting that the precipitate size was

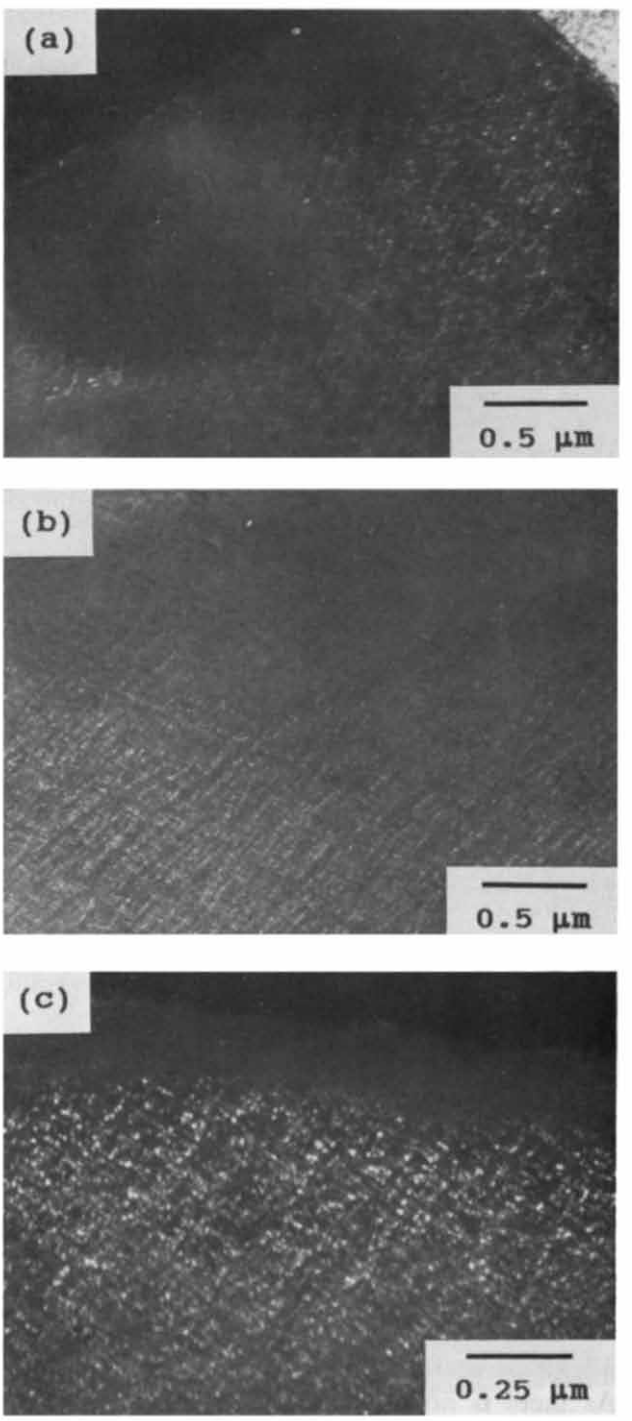

Fig. 7. Transmission electron micrographs (dark field) of selected annealed specimens: (a) AS1; (b) AS4; (c) AS8.

very small and below the critical particle size for transformation to occur.[13]

4 Discussion

The results from the previous sections can be summarized as follows:

(i) From the TEM and XRD observations all coprecipitated compositions studied had a homogeneous distribution of stabilizing cations.

(ii) Twinning was observed for as-sintered specimens with high scandia content by TEM and optical microscopy. The degree and level of twinning decreased with increasing yttria concentration and specimens S6, S7 and S8 with Y_2O_3 content ≥ 6 mol% exhibited no twinning.

(iii) The XRD results are consistent with TEM observations, in that, the as-sintered specimens S1 to S5 (Y_2O_3 content ≤ 5 mol%) which showed twinning were indexed as having tetragonal symmetry. The compositions which showed no twinning (S6–S8) were indexed as cubic.

(iv) The cell volume as determined from XRD results increased with yttria content and these observations are consistent with larger cation size for Y^{3+} compared with Sc^{3+}.

(v) The twinned structure observed in as-sintered specimens S1–S5 disappeared on extended annealing at 1000°C.

(vi) All the annealed specimens were indexed as having cubic symmetry and these results were supported by TEM observations.

(vii) On annealing, the cell volume, in general, increased for higher yttria-containing compositions and decreased for higher scandia-containing compositions.

(viii) Appearance and/or growth of tetragonal precipitates were observed in annealed specimens. The precipitate size and degree of precipitation was higher in S8 and decreased with increasing scandia content.

(ix) No monoclinic zirconia precipitates were observed in any of the as-sintered or annealed coprecipitated specimens.

4.1 Phase equilibrium expectations

As there is no published phase diagram for the ternary system Y_2O_3–Sc_2O_3–ZrO_2 it is necessary to consider the separate Y_2O_3–ZrO_2 and Sc_2O_3–ZrO_2 binary phase diagrams. For simplicity the role of the Y_2O_3–Sc_2O_3 in this investigation is considered as a 'dopant'-ZrO_2 binary system in order to consider the equilibrium phase assemblage. According to various phase diagrams reported for Y_2O_3–ZrO_2 and Sc_2O_3–ZrO_2 systems, all the compositions of the present study were sintered well into the cubic phase field and therefore can be considered to have the cubic structure at the sintering temperature. However, there is a considerable uncertainty in the literature as to the equilibrium-phase assemblage at the annealing temperature of 1000°C for both binary systems.

Yoshimura[4] has compiled a phase diagram proposed by various authors for the Y_2O_3–ZrO_2 system in the zirconia-rich region. If the Y_2O_3–ZrO_2 phase diagram is considered, then, at the annealing temperature, according to the phase diagram proposed by Scott[5] and Stubican *et al.*,[14] the materials were annealed in the tetragonal + cubic (t + c) two-phase region, whereas, according to Ruh *et al.*[15] and Pascual & Duran,[16] the compositions were annealed in the cubic-phase field.

Similarly much uncertainty exists concerning the Sc_2O_3–ZrO_2 system. Eight phases have been reported for the system; seven of which appear in the zirconia-rich region (0–25 mol% Sc_2O_3). Now, considering the Sc_2O_3–ZrO_2 phase diagram, according to Thornber *et al.*[6] the materials of this study at 1000°C were near the (t + c)/c phase boundary, whereas the phase diagram proposed by Ruh *et al.*[7] suggests that they were sintered in the cubic-phase field. Also, for the 8 mol% Sc_2O_3–ZrO_2 composition, the presence of small quantities of an ordered phase designated as the β-phase with the rhombohedral structure has been reported.[17] Badwal[3] and Bannister & Skilton[18] observed this phase for the 8 mol% composition only in poorly mixed oxides. These authors report the disappearance of the β-phase on grinding and refiring or its absence in coprecipitated specimens. In the present study there was no evidence for the existence of the β-phase in the as-sintered or annealed specimens.

In the real situation there would obviously be doubt as to the (t + c)/c phase boundary at the 1000°C annealing temperature for the Y_2O_3–Sc_2O_3–ZrO_2 ternary system resulting from the Y_2O_3 and Sc_2O_3 combined stabilizing effect on ZrO_2. The X-ray diffraction and transmission electron microscopy results reported here are well supported by conductivity studies as a function of time at 1000°C[8] and clearly indicate that all the compositions in the ternary system and 8 mol% Y_2O_3–ZrO_2 are in the two-phase field.

4.2 Twinning, phase transformations and phase assemblage

Two types of phase transformations clearly occur in the Y_2O_3–Sc_2O_3–ZrO_2 ternary oxide system on cooling the materials from the sintering temperature and subsequent annealing. The first phase transformation occurs without any composition change in scandia-rich as-sintered specimens (S1 and S5). The twinned microstructure observed in these materials has been reported previously for both scandia– zirconia[3,11,12] and yttria–zirconia[5,9,10,19] systems. The twinning reported in a composition close to 8 mol% Sc_2O_3–ZrO_2[3,11,12] was observed irrespective of the cooling rate from the heat treatment or sintering temperatures in the cubic-phase field. Lanteri *et al.*,[9] in investigating 7 mol% Y_2O_3–ZrO_2 compositions, observed twinning but only when the specimen was quenched from the sintering temperature (cubic-phase field). Shibata-Yanagisawa *et al.*[10] observed similar twinning for a 4·2 mol% Y_2O_3–ZrO_2 composition. This twinning in Y_2O_3–ZrO_2 has been assigned to the formation of a dopant-rich tetragonal phase and has been referred to as the t'-phase.[9,10] The existence of the high yttria-content tetragonal phase was reported earlier by Scott[5] in rapidly cooled yttria–zirconia compositions (Y_2O_3 content $\approx$ 2–7 mol%), who suggested that the multiply twinned tetragonal phase was formed by diffusionless or displacive phase transition from the cubic (c) phase. This t'-phase has been described as the non-transformable phase, that is, it does not transform under stress. On the other hand, the tetragonal phase which appears in the equilibrium phase diagram (t-ZrO_2) is lower in dopant than the t'-phase, is formed by diffusional processes (cation rearrangement) and can, if retained as a metastable phase at room temperature, transform under stress to monoclinic zirconia. Scott[5] indicated that the t'-phase is metastable and, on annealing for a sufficiently long time in the two-phase field, would decompose into cubic and t-ZrO_2 phases, as expected from the phase diagram. Sakuma & Suto[19] gave a composition of 4–7 mol% Y_2O_3 over which the lenticular t'-phase was formed. Andersson and coworkers[20,21] have shown that the t'-phase is formed only when materials containing less than $\approx$7 mol% Y_2O_3 are heated in the cubic-phase field and quenched.

In an attempt to establish if the absence of t'-phase in yttria-rich specimens (S6, S7 and S8) was a result of slow cooling, specimen S8 of 8 mol% Y_2O_3 + 92 mol% ZrO_2 composition was quenched in air from a temperature (1750°C) well above the (t + c)/c phase boundary. Transmission electron microscopy of this specimen showed no twinned regions, but only t-ZrO_2 precipitates. Figure 8 shows dark field micrographs for specimens S8 (as-sintered) and QS8 (quenched). It appears that the precipitate size in the as-sintered specimen S8 (Fig. 8(a)) is larger compared with that in the quenched specimen QS8 (Fig. 8(b)), which suggests that the precipitates in the as-sintered specimen (slower cooling rate) had a longer period of time to grow during the 'cooling' cycle from the sintering temperature. The results for yttria-rich compositions are consistent with those of other authors in that no twinning (either in slow cooled or quenched specimens) in the Y_2O_3–ZrO_2 system has been reported for compositions close to the (t + c)/c phase boundary ($\sim$8–9 mol%).

Andersson & Gupta,[21] Lanteri *et al.*[22] and Heuer *et al.*[23] have discussed the thermodynamics of both displacive (or diffusionless) cubic to tetragonal and diffusion-controlled phase transformations by constructing T-T-T and free enery versus composition diagrams. Phases which exist at a given temperature and for a particular composition are those which have the lowest free energy. All the materials of the

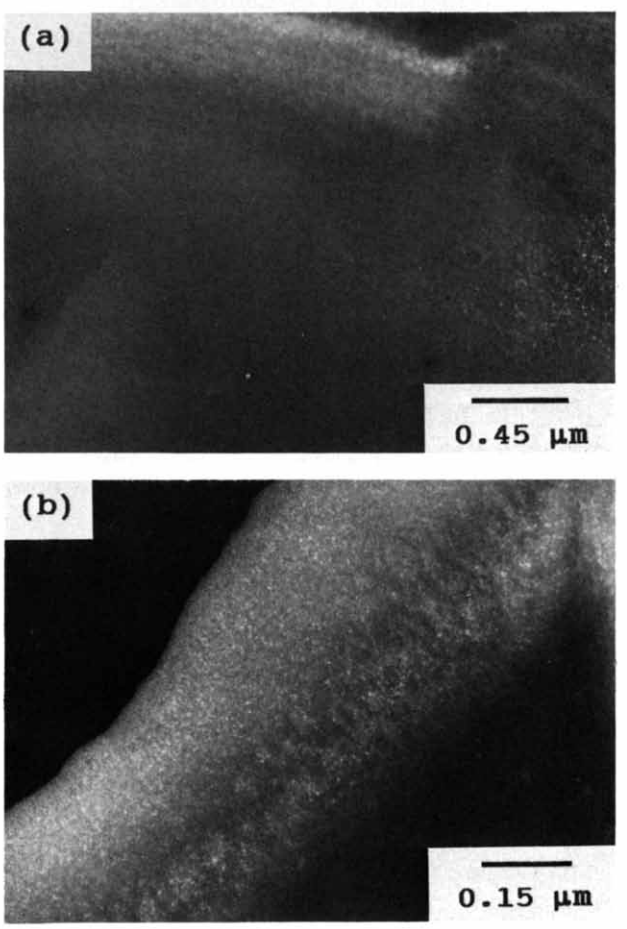

Fig. 8. Transmission electron micrographs (dark field) of 8 mol% Y_2O_3 + 92 mol% ZrO_2 specimens: (a) as-sintered (S8) and (b) quenched (QS8).

present study, at the annealing temperature, are in the (t + c) two-phase region and the free energy of the system will be at a minimum for the two-phase mixture. Heuer *et al.*[23] have discussed that on cooling (from a temperature in the cubic-phase field) a composition in the two-phase field, precipitation of low dopant tetragonal and enrichment of the cubic phase is expected. However, such processes require cation diffusion and changes in the local chemical composition. They are a function of the annealing temperature and take place over a long period of time. Heuer *et al.* argue that if a material is cooled rapidly in the two-phase (t + c) field below a critical temperature without the nucleation of the t-ZrO_2 phase, then the free energy conditions will favour the formation of the t'-phase. Moreover, if precipitation of t-ZrO_2 (a phase with low dopant content) occurs during slow cooling, the matrix will become richer in the dopant and therefore is less likely to transform to the t'-phase. In the displacive transformation, no compositional changes occur and a single variant of the t'-phase is formed consistent with the results reported here. Heuer *et al.*[23] have discussed twinned morphology in terms of a stress relief process which gives rise to mechanical or deformation twinning. The t'-phase nevertheless has higher free energy than the equilibrium two-phase mixture and therefore is metastable in nature and with time decomposes into equilibrium cubic and t-ZrO_2 phases.[22]

The major differences between Y_2O_3- and Sc_2O_3-stabilized materials are that in the Sc_2O_3 counterpart (i) quenching is apparently not required to 'freeze-in' the t'-ZrO_2 phase and (ii) the t'-phase is formed near the (t + c)/c phase boundary. This may be associated with general sluggishness of the phase reactions observed in the scandia–zirconia system.[3,6,11] In the ternary systems Y_2O_3–Sc_2O_3–ZrO_2 naturally there will be a transition with change in the Y/Sc ratio and that may explain the formation of the t'-phase in scandia-rich compositions.

The second phase transformation in these materials is diffusion controlled and occurs as a result of the material being in the two-phase field. The composition of the phases formed is different from the mean composition of the initial phase. In the present study, the t'-phase in scandia-rich specimens S1–S5, like the cubic phase in the as-sintered specimens S6–S8, is in a metastable state and decomposes with time at the annealing temperature. The t-ZrO_2 precipitates form by a diffusional process either directly from the cubic phase (specimens S6–S8) by compositional rearrangement or by the decomposition of the t'-phase for specimens S1–S5 into cubic phase matrix and t-ZrO_2 as required by the equilibrium phase diagram. These observations are additionally well supported by conductivity studies[8] and the observed changes to the cell volume on annealing. The behaviour associated with the annealing processes may be summarized as follows:

(i) For high yttria-containing specimens (AS6–AS8), the cell symmetry was retained but the cubic lattice parameters increased on annealing when compared to the corresponding as-sintered specimens (S6–S8).
(ii) For two scandia-rich specimens (S1 and S2), the cell symmetry changed from tetragonal to cubic and the cell volume decreased on annealing.
(iii) For intermediate compositions (S4 and S5), the cell symmetry change from tetragonal to cubic was accompanied by an increase in the cell volume.
(iv) The cell volume change for specimen S3 was insignificant. In this composition, as a result of the anneal, the lattice parameter a of the tetragonal form increased to the cubic lattice parameter a whilst the tetragonal lattice parameter c decreased.

The point here is, that in all cases on annealing, the precipitation and growth of t-ZrO_2 leaves the matrix richer in stabilizer. In addition for specimens S1–S5 a change in the cell symmetry from t'- to cubic phase occurs. In pure Y_2O_3–ZrO_2 this would cause the cell volume to increase, since the cell volume increases with Y_2O_3 content.[5] In pure Sc_2O_3–ZrO_2 this would cause the cell volume to decrease, since the cell volume decreases with increasing Sc_2O_3 content.[18] In the ternary system, a change is expected from an increase in the cell volume at high Y/Sc ratio to a decrease in the cell volume at low Y/Sc ratio.

Another point worth considering here is the observed line broadening in annealed scandia-rich compositions. Because of the sluggishness of the phase transformation in the scandia–zirconia system, the products of decomposition of the metastable t'-phase may themselves be nonequilibrium phases. Any resulting compositional inhomogeneities with respect to scandia content in the matrix can give rise to the observed line broadening in X-ray diffraction patterns.

5 Conclusions

All the compositions studied have cubic structure at the sintering temperature. On cooling two types of phase transformations occur. The first phase trans-

formation occurs only in compositions between 1 mol% Y_2O_3 + 7 mol% Sc_2O_3 + 92 mol% ZrO_2 (S1) and 5 mol% Y_2O_3 + 3 mol% Sc_2O_3 + 92 mol% ZrO_2 (S5) inclusive. In these materials a dopant-rich tetragonal phase (t') is formed as a result of diffusionless phase transformation from the cubic phase during cooling from the sintering temperature. No compositional inhomogeneities were observed within the grains of this phase. In specimens (S6 to S8) with higher yttria concentration, the t'-phase is not formed. Instead, the high-temperature cubic phase is retained. The t'-phase in scandia-rich specimens S1–S5 and the cubic phase in the as-sintered specimens S6–S8 are in a metastable state. On annealing at 1000°C, a second type of phase transformation occurs as a result of all compositions being in the two-phase (t + c) field. The solute redistribution requires diffusion and rearrangement of cations, and a local change in the chemical composition in all the specimens. This diffusion-controlled phase transformation is dictated by the equilibrium phase diagram and is slow. In scandia-rich compositions (S1–S5), the t'-phase decomposes with time to a cubic phase and t-ZrO_2 precipitates. In yttria-rich specimens, which in the as-sintered state had cubic structures, annealing leads to the enrichment of the cubic phase and precipitation of t-ZrO_2. The precipitate size for an 8 mol% Y_2O_3–ZrO_2 composition (AS8) was determined by TEM to be approximately 60 Å and it decreased with increasing scandia content. In general, the phase transformations in scandia-rich composition were sluggish and yttria-rich compositions had faster kinetics for precipitation and growth.

Acknowledgements

The authors wish to thank B. Terrell for coprecipitation of powders, Dr M. J. Bannister for reviewing the paper and Professor D. J. M. Bevan for many useful discussions. The work described in this paper formed part of FTC's M. App. Sci. at Chisholm Institute of Technology. He would like to thank the course supervisors Drs S. J. Bone and M. J. Bannister.

References

1. Stevens, R., *An Introduction to Zirconia.* Magnesium Elektron Publication, London, 1983, No. 113.
2. Etsell, T. H. & Flengas, S. N., The electrical properties of solid oxide electrolytes. *Chem. Rev.*, **70** (1970) 339–76.
3. Badwal, S. P. S., Effect of dopant concentration on electrical conductivity in the Sc_2O_3–ZrO_2 system. *J. Mater. Sci.*, **22** (1987) 4125–32.
4. Yoshimura, M., Phase stability of zirconia. *J. Amer. Ceram. Soc. Bull.*, **67** (1988) 1950–5.
5. Scott, H. G., Phase relationships in the zirconia–yttria system. *J. Mater. Sci.*, **10** (1975) 1527–35.
6. Thornber, M. R., Bevan, D. J. M. & Summerville, E., Mixed oxides of the type MO_2(Fluorite)–M_2O_3. V. Phase studies in the systems ZrO_2–M_2O_3 (M = Sc, Yb, Er, Dy). *J. Solid State Chem.*, **1** (1970) 545–53.
7. Ruh, R., Garrett, H. J., Domagala, R. F. & Patel, V. A., The system zirconia–scandia. *J. Amer. Ceram. Soc.*, **60** (1977) 399–403.
8. Ciacchi, F. T. & Badwal, S. P. S., The system Y_2O_3–Sc_2O_3–ZrO_2; Phase stability and ionic conductivity studies. *J. Europ. Cer. Soc.*, **7**.
9. Lanteri, V., Chaim, R. & Heuer, A. H., On the microstructures resulting from the diffusionless cubic-to-tetragonal transformations in ZrO_2–Y_2O_3 alloys. *J. Amer. Ceram. Soc.*, **69** (1986) C258–C261.
10. Shibata-Yanagisawa, M., Kato, M., Seto, H., Ishizawa, N., Mizutani, N, & Kato, M., Crystallographic analysis of the cubic-to-tetragonal phase transformation in the ZrO_2–Y_2O_3 system. *J. Amer. Ceram. Soc.*, **70** (1987) 503–9.
11. Summerville, E., Ordered and disordered phases in the zirconia–scandia system. PhD Thesis, The Flinders University, SA, 1973.
12. Drennan, J. & Badwal, S. P. S., unpublished.
13. Garvie, R. C., Critical size effects in alumina–zirconia alloys. In *Advances in Ceramics, Vol. 24A: Science and Technology of Zirconia III*, ed. S. Somiya, N. Yamamoto & H. Yanagida. The American Ceramic Society, 1988, pp. 55–69.
14. Stubican, V. S., Hink, R. C. & Ray, S. P., Phase equilibria and ordering in the system ZrO_2–Y_2O_3. *J. Amer. Ceram. Soc.*, **61** (1978) 17–21.
15. Ruh, R., Mazdiyasni, K. S., Valentine, P. G. & Bielstein, H. O., Phase relationship in the system ZrO_2–Y_2O_3 at low Y_2O_3 contents. *J. Amer. Ceram. Soc.*, **67** (1984) C190–C192.
16. Pascual, C. & Duran, P., Subsolidus phase equilibria and ordering in the system ZrO_2–Y_2O_3. *J. Amer. Ceram. Soc.*, **66** (1983) 23–7.
17. Moghadam, F. K., Yamashita, T., Sinclair, R. & Stevens, D. A., Transmission electron microscopy of annealed ZrO_2 + 8 mol% Sc_2O_3. *J. Amer. Ceram. Soc.*, **66** (1983) 213–16.
18. Bannister, M. J. & Skilton, P. F., The cubic⇌tetragonal equilibrium in the system zirconia–scandia at 1800°C: Effect of alumina. *J. Mater. Sci. Lett.*, **2** (1983) 561–4.
19. Sakuma, T. & Suto, H., Cubic–tetragonal phase separations in Y-PSZ. In *Advances in Ceramics, Vol. 24A: Science and Technology of Zirconia III*, ed. S. Somiya, N. Yamamoto & H. Yanagida. The American Ceramic Society, 1988, pp. 531–5.
20. Andersson, C. A., Greggi, Jr, J. & Gupta, T. K., Diffusionless transformations in zirconia alloys. In *Advances in Ceramics, Vol. 12: Science and Technology of Zirconia II*, ed. N. Claussen, M. Rühle & A. H. Heuer. The American Ceramic Society, 1984, pp. 78–85.
21. Andersson, C. A. & Gupta, T. K., Phase stability and transformation toughening in zirconia. In *Advances in Ceramics, Vol. 3: Science and Technology of Zirconia I*, ed. A. H. Heuer & L. W. Hobbs. The American Ceramic Society, 1981, pp. 184–201.
22. Lanteri, V., Heuer, A. H. & Mitchell, T. E., Tetragonal phase in the system ZrO_2–Y_2O_3. In *Advances in Ceramics, Vol. 12: Science and Technology of Zirconia II*, ed. N. Claussen, M. Rühle & A. H. Heuer. The American Ceramic Society, 1984, pp. 118–30.
23. Heuer, A. H., Chaim, R. & Lanteri, V., Reviews: Phase transformations and microstructural characterization of alloys in the system Y_2O_3–ZrO_2. In *Advances in Ceramics, Vol. 24A: Science and Technology of Zirconia III*, ed. S. Somiya, N. Yamamoto and H. Yanagida. The American Ceramic Society, 1988, pp. 3–20.